

Senior Research

An Investigation in the Specular
Reflectance Characteristics of Substrates
in Electrophotographic Printing

Final Report

Michelle Spampata
Center for imaging Science
Rochester Institute of Technology
May 2006

Copyright © 2006
Center for Imaging Science
Rochester Institute of Technology
Rochester, NY 14623-5604

This work is copyrighted and may not be reproduced in whole or part without permission of the Center for Imaging Science at the Rochester Institute of Technology.

This report is accepted in partial fulfillment of the requirements of the course 1051-503 Senior Research.

Title: An Investigation in the Specular Reflection Characteristics off Substrates in Electrophotographic Printing.

Author: Michelle Spampata

Project Advisor: Dr Jonathon S. Arney
1051503 Instructor: Joseph P. Hornak

An Investigation in the Specular Reflection Characteristics of Substrates in Electrophotographic Printing

Michelle A. Spampata* and Jonathan S. Arney

Center for Imaging Science
Rochester Institute of Technology
Rochester, NY 14623-5604

May 07, 2006

Abstract

It is well known that the choice of paper affects the print quality in laser electrophotographic images. The range of colors (gamut) is a major print quality metric that varies significantly with the choice of paper. Gloss, surface roughness, whiteness, and light scattering are all properties of paper that one might expect to affect color reproduction. Nevertheless, how these paper properties influence color and print gloss is not well understood. The focus of this work is to add to this understanding. This was done through the construction of a feature vector of paper properties. Statistical analysis was applied to these metrics, and the major correlations with printed color gamut were the gloss of the paper and the basis weight of the substrate.

The underlying theory of how light interacts with an inhomogeneous material like paper was also tested. BRDF plots compiled with the micro-goniophotometer at multiple angles of incidence showed that Fresnel's Law was obeyed, and that both coated and uncoated substrates can be treated as homogeneous materials with a single characteristics index of refraction.

Acknowledgements:

I would like to thank my advisor, Dr. Arney, for all of his advice and encouragement in completing this project; my family, who always pushed me to do my best; and lastly, all my friends that helped me survive the day-to-day. The success of the following research would not have been possible without all of your support.

Table of Contents

| | |
|---------------------------------------|------------|
| Copyright Release | ii |
| Abstract | iii |
| Acknowledgement | iv |
| Table of Contents | v |
| 1 Introduction | 1 |
| 2 Background | 2 |
| Substrate Characteristics..... | 2 |
| Light/Substrate Interaction..... | 2 |
| Gloss..... | 3 |
| Gamut..... | 5 |
| 3 Experimental Methods | 6 |
| Hewlett-Packard..... | 6 |
| Feature Vector Formation..... | 7 |
| Statistical Analysis..... | 10 |
| 4 Results and Discussion | 11 |
| BRDF Analysis..... | 11 |
| Densitometry..... | 13 |
| Statistical Analysis..... | 13 |
| Fresnel Validation..... | 15 |
| 5 Conclusions | 16 |
| References | 17 |

1 Introduction

Anecdotal evidence strongly suggests that the color gamut produced by a color laser printer depends on the type of substrate used in a printer. The substrate type has been shown not to affect the amount of toner that reached the final printed page. This indicates that the gamut is influenced by the scattering coefficient, S , within the toner layer and/or by the micro-roughness of the image surface, σ_α . Both of these can be expected to be sensitive to the image-fusing process in an electrophotographic printer, and the substrate properties can be expected to influence this fusing process. However, it previously was not known whether the major gamut-controlling parameter in the toner cartridge was S , or σ_α ; and even less was known about which substrate properties were important in controlling the S and σ_α of the final printed image. The problem is that different ways of measuring roughness do not correlate well, and only approximate correlations have been seen between gloss, color gamut, and various roughness measurements. We applied a statistical pattern-recognition analysis to these measurements in order to add to our understanding of how different surface roughness metrics relate. This report depicts the work that was carried out in order to find these answers, and the answers to questions revealed in the experimental process.

2 Background Optical Characteristics of Paper and Printed Images

2.1 Substrate Characteristics

The origin of the word paper can be traced back to the Greek papyrus.⁶ This is not surprising since papyrus was the first material that was used to make paper. The earliest trace of paper made from papyrus dates back to 3580 B.C.⁷ Paper, or at least the process for modern manufacture, was first developed in China in the year A.D. 105.⁵ Since then paper has evolved and changed into the commodity that it is today.

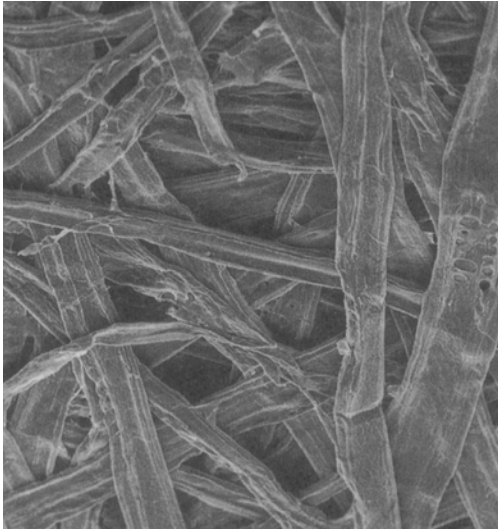


Figure 1 - Scanning electron micrograph of paper surface.⁵

When evaluating any type of print, it is fairly obvious that the properties of the substrate used, play a large role in what it may 'look' like after printing. There are physical (basic weight and grammage, thickness, formation, directionality, two-sidedness, smoothness, and porosity) and optical (gloss, color, opacity, transparency, and brightness) properties of paper⁵. In this study, we mainly looked at grammage, formation, smoothness, gloss, color, and transparency and how they correlate to the final color gamut of the printed image. These properties are important to an imaging scientist because they all effect how light interacts with paper.

2.2 Light/Substrate Interaction

When light strikes the surface of a sheet of paper, three things can happen. Some of the light is reflected back as reflected light; some is absorbed; and the rest is transmitted out the reverse side, as illustrated in Figure 2.

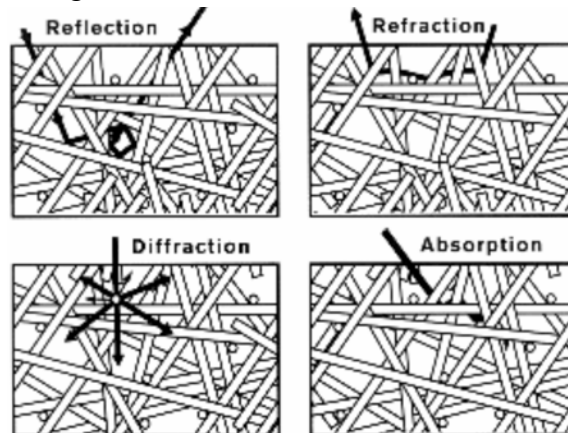


Figure 2 - Diffuse reflection, refraction, diffraction, and absorption of light inside of paper⁹

The light that is reflected from a paper or a printed image can be divided into two types: volume scattered light and specular light. The volume scattered light is that component of the reflected light that has penetrated into the bulk volume of the paper prior to reflection. This component of the reflected light is diffused laterally across common papers for distances of 10s to 100s of microns. It is also dispersed over a very broad range of angles from the surface.¹³ Volume reflected light often behaves as Lambertian light, and it is the light that carries most of the color and texture appearance of the paper or a printed image.

The specular component of reflected light is the light that is reflected at the air/surface interface in accordance with Fresnel's Law. The specular component is reflected at an angle that is equal to, but opposite from the angle of incidence, as seen in Figure 3.

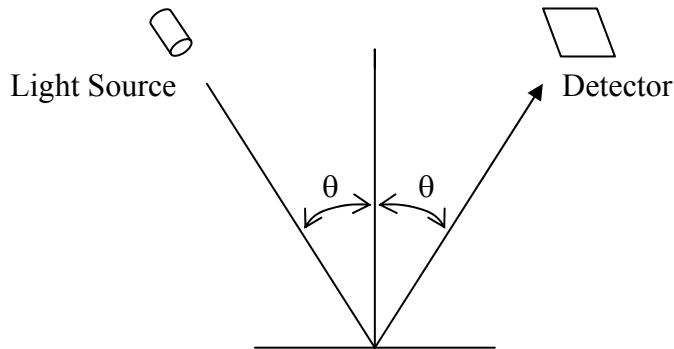


Figure 3 – Demonstration of Equal/Opposite angle

It is not significantly dispersed in lateral dimensions, and it is typically dispersed over a relatively narrower range of angles around the equal/opposite angle. It is this component of the reflected light that is responsible for gloss characteristics of a paper or printed image.

2.3 Gloss

Gloss refers to the visual attribute of specularly reflected light while specular reflection refers to the light measured instrumentally.³ Gloss is the bright shine that results from holding glossy objects at a particular angle relative to a light source.⁴ The term "gloss" is intuitively familiar as a phenomenon that increases the color value and decreases the chroma of printed images. A high gloss printed page is rendered unreadable if held in a way that shows the gloss to the reader.⁹ However, high-gloss images are typically perceived to have higher color saturation. This apparent contradiction is the result of the relatively narrow angular distribution of high gloss light that allows the reader to direct the gloss away from the field of view, thus avoiding the loss of chroma associated with specular reflections.

It has been shown that gloss is strongly related to the roughness of the surface. In general, the smoother the surface is, the higher the gloss is. An extremely rough surface can diffuse specular light over such a broad range of angles about the equal/opposite angle that it takes on an appearance that is very much like that of bulk volume reflected light.⁹ A very broad angular distribution of specular light is perceived as low gloss, and also gives a low gloss index when measured with a standard gloss meter. This is illustrated in Figure 4.

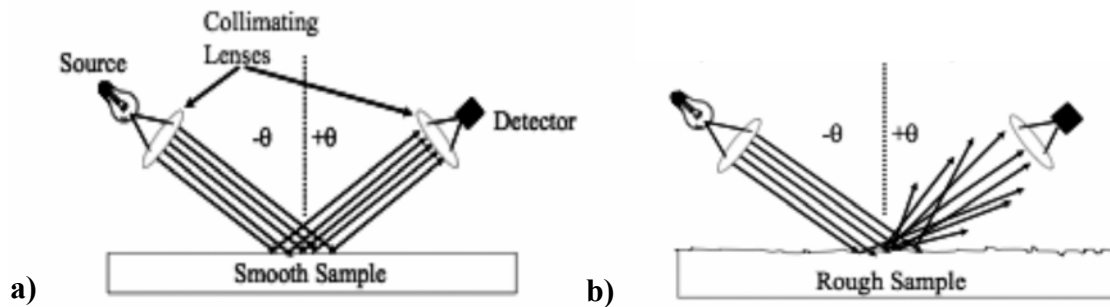


Figure 4 – The behavior of a standard gloss meter with collimating lenses.¹⁰

Another visual attribute of gloss that is typically found to be objectionable in a printed image is gloss variation. Since uneven gloss is perceived as poor quality, the gloss variation is an important attribute of printed images. Figure 5 illustrates an imaging system developed at RIT that is useful for measuring gloss variation.² Moreover, this instrument can measure specularly reflected light over a wide range of reflection angles around the equal/opposite angle. A graph of reflected light versus angle is called a bi-directional reflection distribution function, BRDF.³

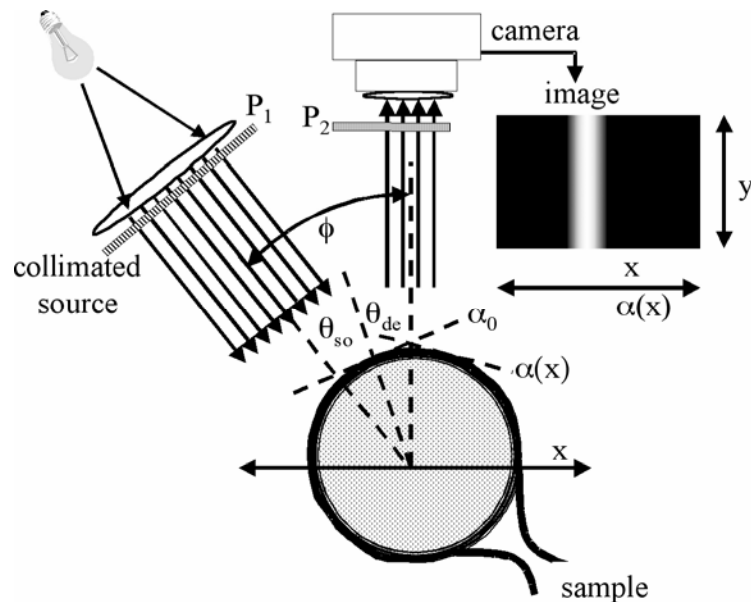


Figure 5 - RIT Micro-Goniophotometer²

There are three ways to measure a BRDF, as illustrated in Figure 6. One way is to scan the detector around the equal/opposite angle (Fig. 6(A)), and another is to scan the light source (Fig. 6(B)). The device in Figure 4 generates a BRDF as the reflected light versus the tilt angle, q , of the sample surface. This is illustrated in Fig. 6(C).

The BRDF measured, as shown in Figure 6(B) and later in Figure 9, provides a direct measure of the distribution of surface angles.³ In addition, the device shown in Fig. 5 allows a scan in the vertical direction, and this gives a direct measure of the spatial variation of specular

light. Thus, both spatial and angular distributions of specular light were measured in this project.

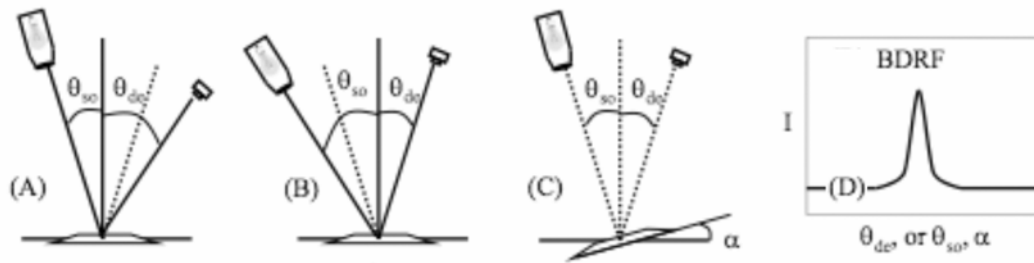


Figure 6 - A goniophotometer measures reflected light as a function of (A) angle of detection θ_{dc} , (B) angle of illumination θ_{so} and/or (C) surface tilt angle α , resulting in a (D) BRDF curve.¹⁰

2.4 Gamut

When evaluating the overall quality of printed color images, color appearance is an important part of image quality. If the color does not look right, other image quality parameters might not matter, and the print could be considered to be low in quality. The color gamut is the range of colors that can be displayed in a printed image, typically measured as a volume in color space. It has been shown that the color gamut, as expected, increases as the gloss of the image increases. This effect is quite evident with color laser images. Anecdotal evidence seems to indicate that the choice of substrate can have a significant impact on color quality for a given color laser printer. However, it is not known what characteristics of papers most influence the final gloss and color gamut of printed images. This study was undertaken to understand the relationship between substrate properties and the color gamut of printed color laser images.

3 Experimental Methods

3.1 Hewlett-Packard

For this study, Hewlett-Packard has donated eleven substrate samples that had been used to generate color laser images on a high-quality, desktop color printer. The samples, as identified by HP, are shown in the following table. Typical paper metrics are included for the sheets. The "Type" category was assigned by HP according to gloss level, but quantitative gloss numbers were not supplied.

Table 1 - The eleven paper samples that will be used in this study. The parameters shown were measured by Hewlett-Packard

| | Name | Type | Brightness | Weight (lbs) | Grammage (g/m ²) | Gamut (CIELab) |
|---|---|------------------|------------|--------------|------------------------------|----------------|
| • | HP Glossy Photo and Imaging Laser Paper | Glossy | 95 | 32 | 120 | 445500 |
| ▪ | HP Color Laser Paper Heavyweight | Matte | 96 | 28 | 105 | 352000 |
| • | HP Matte Brochure Paper | Matte | 96 | 43 | 160 | 385000 |
| ▪ | HP Multipurpose Paper | Matte | 90 | 20 | 75 | 302500 |
| ▪ | HP Multipurpose Paper | Matte | 92 | 20 | 75 | 302500 |
| ▪ | HP Digital Copy | Matte | 84 | 20 | 75 | 266750 |
| • | HP Brochure Paper -Two Sided | Glossy/ Matte | 97/ 112 | 44 | 160 | 453750 |
| ▲ | HP Presentation Paper | Soft Gloss | 107 | 32 | 120 | 434500 |
| | HP Color Laser Photo Paper | Glossy | | | 220 | 420750 |
| ▲ | HP Cover Paper | Matte | 112 | 75 | 200 | 371250 |
| | Office Max MaxBrite Copy Paper | Matte | 84 | 20 | 75 | 275000 |

▲ - HP Color Laser Paper • - HP Specialty Paper ▪ - HP Paper

Hewlett-Packard printed color test images on each of the eleven paper samples using a color laser printer. The printer was a proprietary test printer used by HP as a typical example of a high quality laser printer. HP reported operating the printer with the fuser speed and temperature set for each individual paper sample at what HP reported as the optimum for that sheet. HP measured the printed color gamut and the other metrics shown in the table. As will be shown, there is evidence to indicate that the fuser was not in fact at an optimum setting with regard to color gamut.

3.2 Feature Vector of Substrate

The feature vector of the substrate needed to be compiled. We used physical and surface metrics to accomplish this.

3.2.1 Physical Metrics

The *density distribution* (paper formation) was not measured directly in this study; rather, the optical density was measured in transmitted light with a transmission microdensitometer. Here we looked at the substrate optically to determine what the structure and formation of the paper looked like.

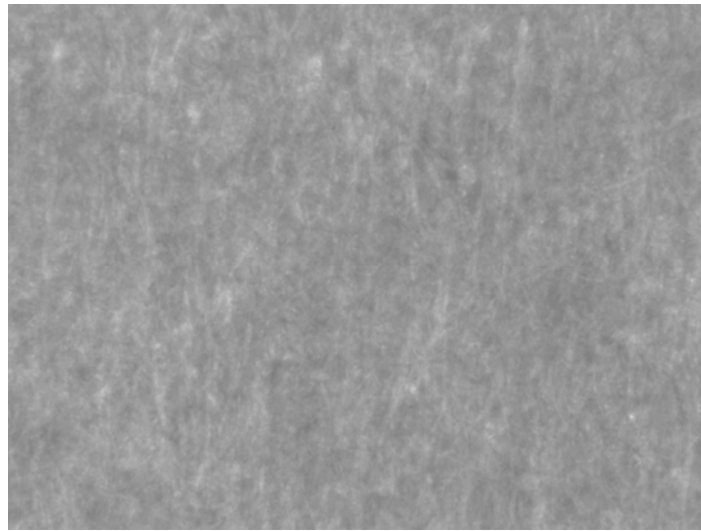


Figure 7 – Image taken with transmission microdensitometry.

A microdensitometer was used with back lighting, and an image was captured that shows the spatial variation in the transmittance of the paper. The moments of the probability density distribution of the transmittance were extracted as metrics of spatial noise. In addition, Fourier analysis was applied to determine the correlated nature of this noise.

The grammage of the paper was used to calibrate the optical density measurements to variation in the *mass density*. For all of the samples the grammage is already known.

$$D = \frac{\textit{grammage}}{\textit{thickness}}$$

3.2.2 Surface Metrics

Raking angle illumination can be used to characterize the roughness of the substrate, as seen in Figure 8. Here an image was captured with illumination at a low angle to the surface. When this angle is too low, shadows can cast over the sample. When it is too high, there would be a lack of variation in the sample. Some experimental trial-and-error was required to

determine the optimum conditions for analysis of the samples. Given that the system was linear the images were flat-fielded to overcome an unavoidable problem with uneven illumination.

In order to determine how the paper properties affect the final printed image, the *BRDF gloss* was determined. Here using the goniophotometer, we compared irradiance vs. angle and gloss variation vs. angle. The goniophotometer is shown in Figure 5. A sample of substrate was wrapped around a 15 mm cylinder and illuminated with collimated, polarized light. An image of the sample was then captured with a CCD camera, also behind a polarizer to filter out specular light from diffuse light.⁴

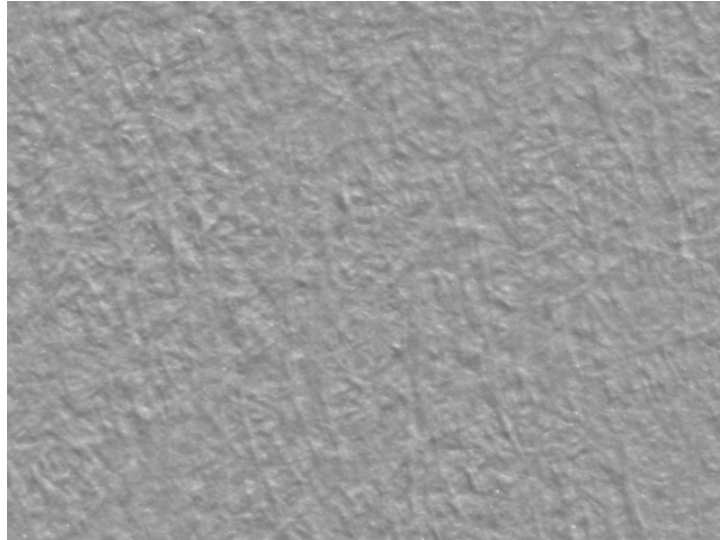


Figure 8 – Image taken using raking angle illumination

The illumination angle, θ_{so} , and the detection angle, θ_{de} , are held constant. The x direction of the captured image is the change in the tilt of surface angle, α . The horizontal image location, x , can be converted into mean tilt angle of the sample, α , by using the equation below, where r is the radius of the cylinder.⁴

$$\alpha(x) = \sin^{-1}\left(\frac{x}{r}\right)$$

By scanning the x direction of the captured image, and by calibrating the camera to radiometric units, a BRDF is generated for a given sample. An example of this is shown in Figure 9.

In the example image in Figure 9, the specular band is clearly visible, and its angular distribution can be calculated from the known geometry of the cylinder. A horizontal scan of the image yields its' respective BRDF. The specular curve is centered at $\alpha=0$, where the specular reflection from the sample is at a maximum. This is visible as the peak in the BRDF.

When a BRDF is measured by scanning across the source or detector angles, as is done with a traditional goniophotometer, each point on the BRDF corresponds to a different Fresnel specular angle, θ in Figure 6. By measuring reflectance versus sample angle, α , however, the

resulting BRDF represents the angular distribution of light at a single, fixed specular angle, θ . As a result, the shape of the specular curve in Figure 9 is a function of only the topography of the sample, and the area under the curve is proportional to the total Fresnel reflectance.^{2,3} This was experimentally demonstrated to be true in both coated and uncoated substrates.

This micro-goniophotometric system allows a simultaneous measurement of reflectance at different sample angles, α . Roughness in the surface topography spreads out the specular curve over some width in the α direction. This is very useful to characterizing gloss because it incorporates an additional metric, σ , the RMS deviation about the mean specular angle, α , to knowledge of the substrates themselves.

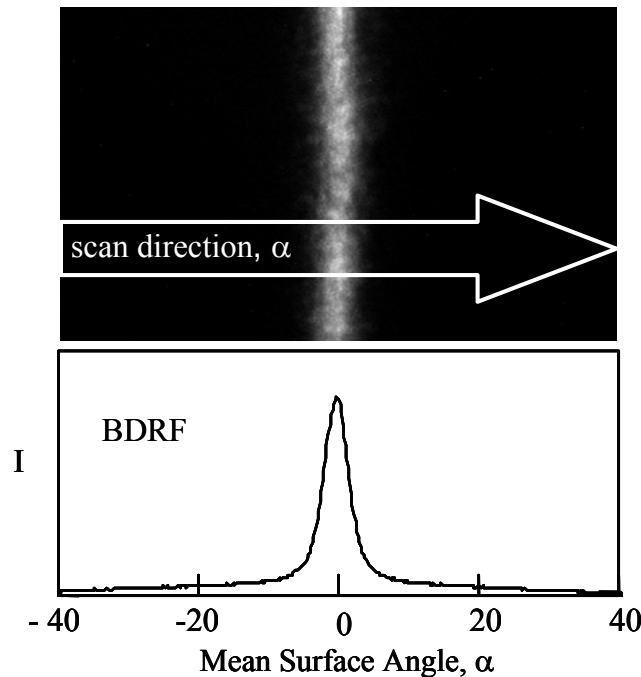


Figure 9: Illustration of a captured image and its respective, BRDF, generated by the micro-goniophotometer depicted in Figure 5.

In order to compare irradiance vs. angle and gloss variation vs. angle, the existing micro-goniophotometer was used to measure the BRDF and RMS Granularity curves of 11 different samples of printable substrate. The variety included matte, soft gloss, and glossy substrates of multiple grammage and brightness. Angle is the angle, α , relative to the peak. I is the irradiance which is the BRDF magnitude at each α . Gloss variation is the RMS deviation at each angle. The latter was measured by calculating the RMS deviation in each vertical column of the BRDF images illustrated in Figure 9.

High repeatability was demanded from this project. The intensity of light emanating from the fiber optic source had to remain constant throughout the experiment, along with the f-stop setting on the camera lens. The micro-goniophotometer was bolted down to an optical bench to ensure that none of the necessary parts moved during the experiment. Additionally, initial calibration/characterization data was taken and used as reference throughout the study to make sure these ‘constants’ were unchanged.

For each substrate sample, two images were captured; these will be referred to as the “light” image and the “dark” image. The light images were captured with the P₁ and P₂ polarizer’s aligned in parallel so that a maximum amount of light was let through to the CCD. The dark images were subsequently captured with the polarizer’s crossed.

A difference image for each substrate sample was generated, by subtracting the dark image from the light image. The difference image contains only light which maintains polarization when reflected. The diffuse, bulk scattered light can thus be eliminated from future measurements, leaving only specular light. Difference images for each sample were scanned in the x direction. As previously mentioned, this yields the BRDF for that particular substrate, varying with sample angle, α . Each BRDF yielded by the micro-goniophotometer in this experiment was analyzed in a previously demonstrated MathCAD algorithm for nine statistical metrics, in vector form:

$$V_{feature} = \begin{bmatrix} A \\ w_{1/2} \\ w_{1/3} \\ w_{1/10} \\ h \\ \sigma_{max} \\ \sigma_{BRDF} \\ sk \\ Ku \end{bmatrix}$$

where A is the area under the BRDF curve (P vs. α), $w_{1/2}$ is the peak width in degrees at half the peak height, $w_{1/3}$ is the peak width at h/3, $w_{1/10}$ is the peak width at h/10, h is the peak height, σ_{max} is the RMS deviation of the pixel values in the column at the peak angle ($\alpha=0$), σ_{BRDF} is the second moment of the BRDF about angle $\alpha=0$, sk is the skewness, and ku is kurtosis of the BRDF.

The primary goal of collecting nine statistical metrics is to have a detailed set of quantitative measurements for each BRDF curve, and in turn, these metrics were used to determine the influence that the properties of the substrate have on printed images. The substrates’ BRDF can then be statistically grouped by similarity of their nine metrics, and hypothetically, these groupings will signify some known physical property of the substrate that correlates with the output gamut.

The gloss of each substrate was also measured with a standard gloss meter at 20°, 60°, and 85°.

3.3 Statistical Analysis

The last part of this study is to do a statistical analysis on the data. For this a collaboration was formed with Dr. Peter Anderson of the Computer Science department and Dr. Marcos Esterman of the Industrial & Systems Engineering department. The BRDF and gloss granularity functions produced by the micro-goniophotometer were used to construct a feature

vector of surface characteristics. Similarly, transmission microdensitometry was used to produce a feature vector of mass density. The two feature vectors were combined into a single substrate feature vector. Additional standard characterization properties, such as grammage (g/m^2), were also included. Pattern recognition procedures, with the software package MiniTab, were used to search for correlations between the substrate and the gamut volume.

4 Results and Discussion

4.1 BRDF Analysis

Using the micro-goniophotometer, four independent trials were run on each of the eleven samples of paper along with a known reference paper. Results from the reference paper served to establish the experimental precision of the analysis and enabled a calibration of the instrument for day-to-day comparisons. The images captured were analyzed using an algorithm that computed key metrics that are determined from the BRDF. Some of the features that we have found to be generally useful are the area under the BRDF, the height of the BRDF peak, the width at 1/2, 1/3, and 1/10 of the BRDF peak, the RMS deviation at the peak height when scanned along the y-direction (Figure 4), skewness, and kurtosis.

Since the area under the BRDF curve represents the Fresnel reflectance, and the height is influenced by the surface roughness, looking at area vs. height is fundamental in distinguishing gloss difference due to surface roughness, σ_α , and gloss differences due to index of refraction, n , and to multiple layer effects.³ Figure 10 shows the area under the BRDF (controlled by n , and multiple layers) vs. the peak height (controlled by σ_α) for the paper samples in this project.

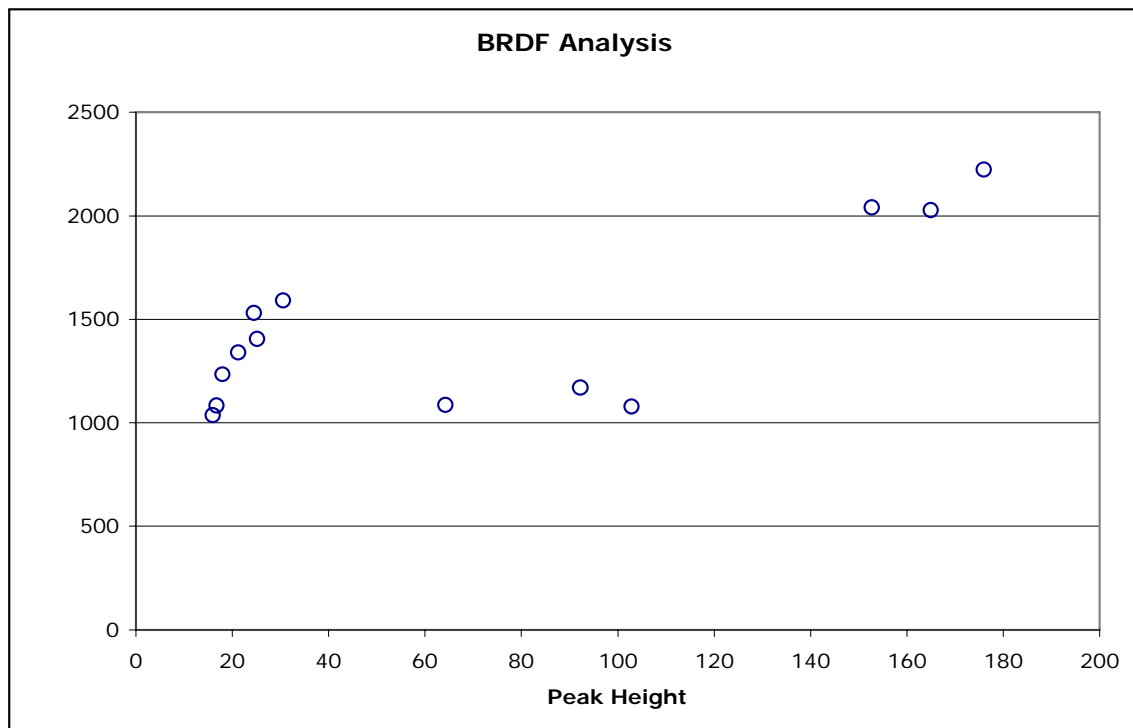


Figure 10 – Micro-Goniophotometer Trial 2

In looking at the graph, there are three distinct clusters. The one on the left represents the substrates labeled as matte. These are so-called "plain papers" without a surface coating. They are incapable of sub-surface, multiple layer effects, and their variation in area, A , is a manifestation of a variation in the effective index of refraction of the samples. The cluster on the right represents high gloss samples with clear overcoats on top of smooth paper. These samples are both very smooth (high h value) and have BRDF areas that are approximately twice that of the matte cluster, which indicates the sub-layer specular effect. The cluster in the middle represents three samples of so-called "soft gloss" paper. These are papers coated with a smooth, but opaque coating, thus giving a relatively high gloss without sub-surface specular reflections. These results are entirely consistent with previous work that shows that BRDF peak width is governed primarily by surface roughness while area is governed by refractive index, n , and multiple layer reflections.²

In addition to the BRDF, measurements were made of the RMS deviation, σ , for scans made in the y direction, as shown in Figure 4. Values of σ were plotted versus the horizontal α direction, and peaks similar to the BRDF were observed. The relationship between the BRDF and the σ vs. α function were studied in a project conducted by Ms Ling Ye, a co-worker in this laboratory. From the results of Ms Ye's study, it became evident that the BRDF and the σ vs. α function are related, and that the typical paper sample and laser printed sample is composed of two spatially distinct surface regions: one that is relatively smooth and low frequency, and the other that is rougher and of higher frequency. The two regions provide a rationale for the high, positive kurtosis observed in all of the measured BRDFs.

4.2 Densitometry

Another part of the feature vector consists of microdensitometry measurements. Here transmission densitometry was used as a method for estimating the random distribution of mass (called paper formation). Raking angle illumination was used to measure the surface roughness of the paper. The design and assembly of a microdensitometer was undertaken to make measurements seen in Figure 7 and 8. This system needed to be able to make both of the measurements using the same area of each substrate. This was achieved by making sure that the planar and point sources used for the transmission and raking angle measurements were each fastened to make sure that the geometry did not change. This also helped achieve repeatability. Another goal of the microdensitometry system was to try to achieve even illumination across the raking angle measurements. Using the point source, this was not achievable, but since the system was linear with respect to light flux, correction for this was achieved by applying a low-pass filter to remove the highest frequencies. This low-passed, blurred image was then used as an illumination reference image to flat field the experimental images. Flat fielding was done by dividing the experimental image by the reference, and then multiplying by the mean of the reference. The mean and standard deviation was then calculated to form the metric used in the feature vector, $\frac{\sigma}{\mu}$. These computations were completed with ImageJ.

4.3 Statistical Analysis

The final feature vector used to find a correlation between the gamut and the properties of the substrate consisted of the following fifteen parameters: A- area under the BRDF; $w_{1/2}$ – width at half the peak height of the BRDF; $w_{1/3}$ – width at a third of the peak height; $w_{1/10}$ – width at a tenth of the peak height; h – peak height of the BRDF; Sk – skewness; Ku – kurtosis; σ_a and σ_b – parameters explaining facet theory; RA – raking angle illumination metric; T – transmission microdensitometry metric; G20, G60, G85 – standard gloss meter measurements at relative angle in degrees; and Gr – grammage in g/m^2 .

Using the software package MiniTab, numerous first order regressions were experimented with. Basic linear regression using just two metrics to predict the resultant print gamut achieved an r^2 value of 0.86. Backwards elimination was the most successful multiple linear regression technique. In this analysis, all of the predictors in the feature vector are used. Then the value that has the largest P value is removed, and the model is refitted. Each step removes what is thought to be the least significant variable in the model. All variables remaining in the final model had P values less than 0.10. This model achieved a r^2 value of 0.916 but consisted of seven metrics, which is fairly complex.

These values show that there was correlation taking place but not at the level that was anticipated. At this point, intuition was used to form our own model. We know that gloss has an effect on the gamut, and so it was included. The gloss metric used in this work was the ratio of the BRDF width to the height, $GL = w_{1/2}/h$. Testing this metric along with multiple orders of the other metrics, the following model was found which had an r^2 value of 0.96 (Figure 11):

$$\text{Gamut} = a_0 + a_1 \cdot \text{Gr}^{-1} + a_2 \cdot \text{Gr}^{-2} + a_3 \cdot \text{GL}$$

Here Gr is the grammage of the paper (grams per ream).

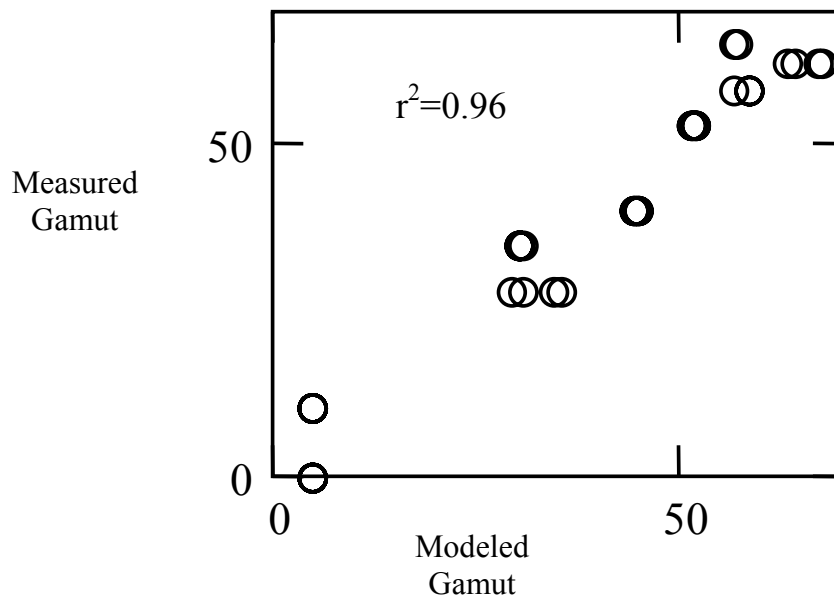


Figure 11: Correlation between Modeled and Measured Gamut.

This result was surprising because if the problem could have been solved this easily this study would not have taken place. When looking at a comparison of the measured gamut and the grammage for each substrate (Figure 12) there appears to be an optimum behavior occurring.

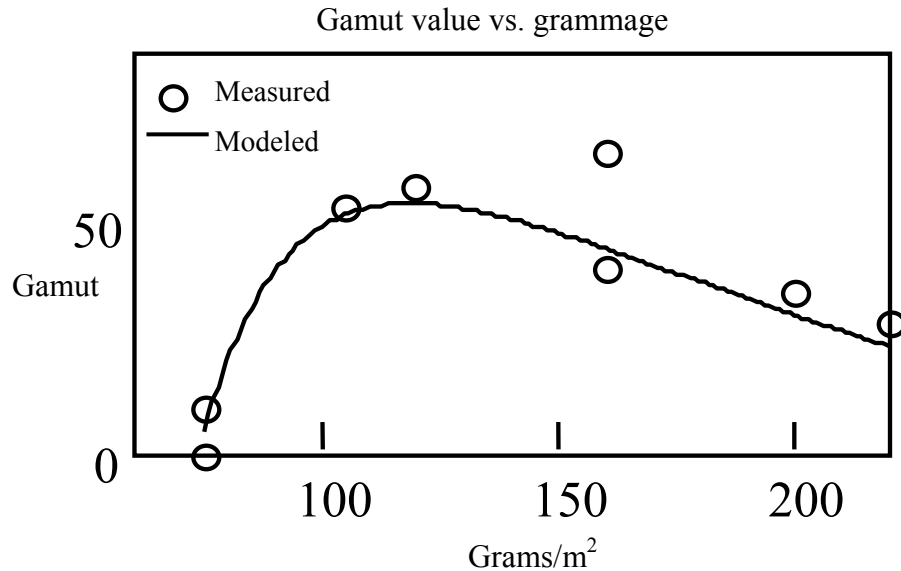


Figure 12: Comparison of Gamut and Grammage.

Figure 12 shows that extremely heavy and extremely light papers show lower gamuts than more commonly used papers. This seems to indicate that the so-called "optimum fuser" setting for very heavy and very light papers may not in fact be optimum with regard to color gamut. Further discussion with HP seemed to indicate that it has more to do with efficient operation of the printer and avoidance of operating artifacts such as offset and sticking. Fusing is the key printer factor that governs gloss, and thus gamut; and fusing is an energy transfer process. It appears to work less efficiently at the high and low extremes of paper size in the particular test printer used in this study.

4.4 Fresnel Validation

The specular component of reflected light is the light that is reflected at the air/surface interface in accordance with Fresnel's Law. Interpretation of measurements during this study assumed Fresnel's Law. However, Fresnel's Law assumes an interface between two homogeneous materials, and paper is quite inhomogeneous over distances that are long, relative to the wavelength of light. Thus, one might reasonably question whether a complex, inhomogeneous material such as paper would behave in accordance with Fresnel's Law

As part of an overall effort to understand the optical mechanisms behind the specular BRDF, Fresnel's Law was tested by measuring the areas of the BRDF versus the incident angle for p - polarized light. In doing this, the micro-goniophotometer was used by varying the degree of the incident angle of light from $\sim 12.5^\circ$ - 90° (Figure 13).

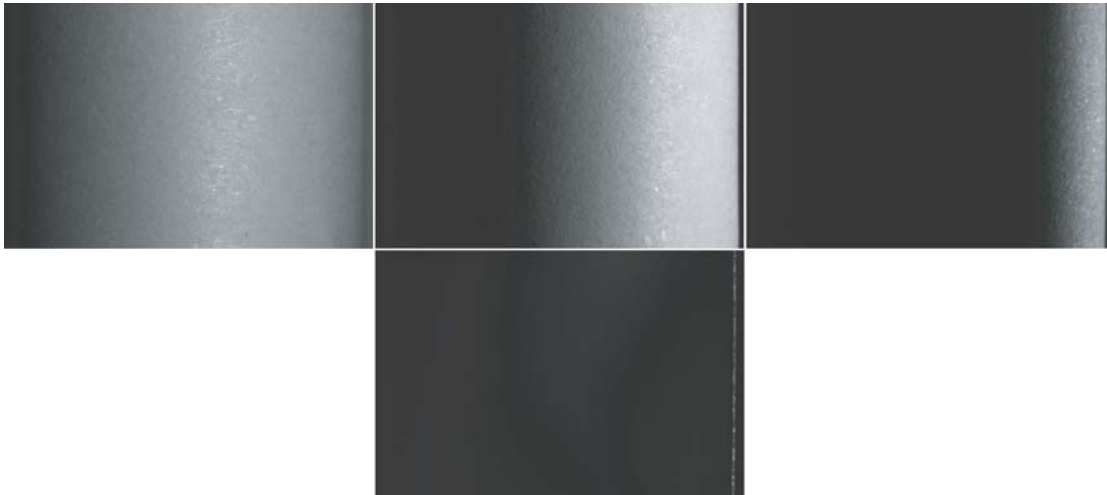


Figure 13 – Images taken with the micro-goniophotometer with illumination angles of 12.5°, 45°, 60°, and 82.5°.

Each image was analyzed in the same manner as the micro-goniometric measurements made previously. The areas of the BRDFs were measured relative to a material of known reflectance and refractive index. From these measurements, the specular reflectance values were calculated and plotted versus the angle of incidence of the light, as shown in Figure 14. Also shown in Figure 14 is a line calculated from Fresnel's Law with an assumed index of refraction, n . The value of n was adjusted to provide a reasonable fit between the model and the data, judged visually. The line shown in Figure 14 was calculated with $n=1.33$. Similar results were found for other papers, both coated and non-coated, with refractive indices ranging from 1.33 to 1.5. Individual substrate papers behave as if they had one effective index of refraction. This indicates that papers can be treated as if they have one homogenous surface, and the theory behind the micro-goniophotometer is sound for coated and uncoated substrates.

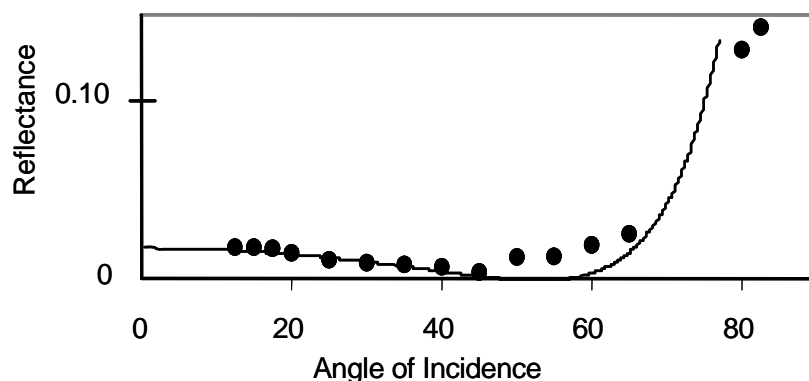


Figure 14 – Examination of Fresnel's Law for Paper illuminated with p-polarized light.
 ● experimental area of the BRDF. — Fresnel's Law calculated with $n=1.33$.

5 Conclusions

Although confounded by the grammage effect, the results of this work clearly show that the gloss of the paper does have a significant impact on the gamut of the printed image. Since energy transfer is so important in achieving good fusing, and thus high print gloss, it is possible that the effect of paper gloss is less of an optical effect and more of a surface roughness effect. Then one would expect a smoother printed image of higher gloss to produce the better gamut. Confirmation of this mechanism is underway currently with a second study being done in collaboration with HP in which the paper samples are being printed and fused with a range of temperatures and speeds. The intent is to quantify the way in which fusing variables and paper variables interact to govern the final print gamut.

An additional, but unanticipated conclusion from this work concerns the way light reflects specularly from papers. It appears that both coated and non-coated papers behave like homogeneous materials with characteristic values of refractive index, with polarized reflections described by Fresnel's Law.

Literature Cited

1. Anderson, M.; Norberg O.; Kruse, B. "The influence of paper properties on color reproduction and color management"; Presented at the Final program and proceedings of IS&T's NIP19: International Conference on Digital Printing Technologies, New Orleans, Louisiana, Sept./Oct., 2003; p 565-569.
2. Arney, J.S.; Hoon Heo. "A Micro-Goniophotometer and Measurement of Print Gloss", *J.Imag.Sci. & Technol.* 2004, 48, pp 458-463.
3. Arney, J.S.; Anderson, P.G.; Pfeister, W. "Color Properties of Specular Reflections", in press, *J.Imag.Sci. & Technol.* 2006. 50.
4. Wible, J.P; "Specular Reflectance of Substrates Used in Printing"; B.S.Thesis: RIT. 2005.
5. Scott, W.E.; Abbott, J.C.; Trosset, S.; "Properties of Paper: An Introduction", Second Edition; Tappi Press: Atlanta, GA, 1989; pp 2, 89-109, 141,
6. Abate, P.R.; ed. *The New Oxford American Dictionary*; Oxford University Press: New York, 2002.
7. Maddox, H.A.; "Paper"; Sir Isaac Pitman & Sons: London, 1936; pp 2
8. Farnand, S.; Töpfer, K.; Kress, W.; Martinez, Ó.; McCarthy, A.; Shin, H.; Zeise, E.; Gusev, D.; "Update on the INCITS W1.1 Standard for Evaluating the Color Rendition of Printing Systems". PICS 2003: The PICS Conference, An International Technical Conference on The Science and Systems of Digital Photography, including the Fifth International Symposium on Multispectral Color Science, Rochester, NY; May 13, 2003; p. 104-107;
9. Nyström, D. "Paper Optics – Part 1"
10. Arney, J.S.; Ye, L.; Banach, S. "Interpretation of Gloss Meter Measurements", Submitted to *J. Imag. Sci. & Technol.* Winter, 2005-06
11. Yang, Li, Kruse, B. "Ink penetration and its effects on printing". *Color Imaging: Device Independent Color, Color Hardcopy, and Graphic Arts V*(Proceedings of SPIE Volume 3963), San Jose, CA; 2000; p. 365-375;
12. Klamann, M. "Colour Rendering Aspects in Digital Printing". TAGA, San Diego, CA; May 2001; 23pages.
13. Arney, J.S.; Arney, C.D.; Katsubae, M.; Engeldrum, P.G.; "An MTF Analysis of Paper", *J.Imag.Sci. & Technol.* 1996, 40, 19.